European Journal of Molecular & Clinical Medicine
ISSN 2515-8260 Volume 08, Issue 01, 2021

Influence Of The Ultrasonic Irradiation On Characteristic Of The Structures Metal-Glass-Semiconductor

O.O. Mamatkarimov[1], B.H. Kuchkarov[2], N.Yu.Sharibaev[3],A.A.Abdulkhayev[4]

[1] *Namangan engineering-technological institute, Namangan, Uzbekistan.*
[2] *Namangan State University, Namangan, Uzbekistan.*
[3] *Namangan engineering-technological institute, Namangan, Uzbekistan.*
[4] *Namangan State University, Namangan, Uzbekistan.*

Abstract:* *The studied influence ultrasonic irradiation on change the rolling charge built-in in structure lead borosilicate glasses PbO - SiO_2 - B_2O_3 - Al_2O_3 - Ta_2O_5. It is shown that influenc ultrasonic irradiation brings about reduction of the rolling charge and improvement insulation parameter glass.

Keywords: Lead-borosilicate glasses, ultrasonic irradiatiation, C-V characteristics, and relaxation.

1. INTRODUCTION

The structures of the type metal - insulator- semiconductor (MIS) on base silicon at present are a base of the broad class semiconductor instrument and structured element of the integral schemes. Herewith, features of the border of the section, semiconductor - insulator, being the most sensitive to external influence, can render the essential influence upon parameters made instrument and structured [1]. The studies of the, on parameters of the borders of the section, such influence as termal processing and ionizing irradiation is denoted it is enough much works[2]. As to influences ultrasonic influence, that available given not it is enough are broadly [3]. So, in work is shown that ultrasonic influence can bring both to reduction, and to increase the charge, localized on interphase border section [4]. In work is shown, ultrasonic irradiation brings about realignment tense valence relationships on hiding border of the section [5], with simultaneous increase the section of the seizure localized electron on them[6]. Lead-borosilicate glasses are free from these shortcomings. Moreover, use of fusible lead borosilicate glasses permit to combine and simplicity of dielectric coverings obtaining[7]. From this point of view, research of the nature of electrophysical processes taking place in the lead - borosilicate glasses coverings under external [8].The purpose persisting work was study of the influence of the ultrasonic influence on value of the rolling charge, available in structure leaden – a boron – a silicate glass[9].

2. MATERIALS

The test structures were fabricated by applying glass to a Si, n-type conductivity substrate, with a crystallographic orientation of <100>. The glass was applied by electrophoresis from a suspension containing a fine-dispersed glass batch (SiO_2-PbO-B_2O_3-Al_2O_3-Ta_2O_5) and isopropyl alcohol, followed by reflow at a temperature of 670-680 degrees in Celsius and annealing in an oxygen-free atmosphere. The thickness of the obtained glass layers was d = (2 ± 0.2) $\pm 10^{-4}$ cm. The mass content of the oxides included in the glass was: SiO_2 - 30%; PbO-50%; B_2O_3 -15%. The investigated glasses also contained aluminum and tantalum oxides with mass fractions of 5% and alkali metal oxides of Na_2O and Na_2O whose mass fractions did not exceed 0.01%[10].

MIS structures were made by vacuum deposition of aluminum on the surface of the glass layer[4]. The diameter of the control electrodes is 3 mm. The structures were subjected to irradiation with longitudinal ultrasonic waves at a frequency of 2.5 mHz with a power of 0.5 W, for 40 minutes, i.e. An effect similar to that described in was used[11]. The acoustic line between the piezoelectric transducer and the structure under study was a liquid[12].

3. METHODS

The method of isothermal relaxation of the capacitance of the metal-insulator-semiconductor (MIS) structure in the process of increasing the charge of the inversion layer was used as the main research method. In accordance with the generally accepted model of the MIS structure, the time dependence of the capacitance of this structure, after the impulse increase of the applied voltage, (without taking into account the influence of the forming charge of the inversion layer) can be expressed by the following relation:

$$C(t) = \frac{\varepsilon\varepsilon_0 K C_D}{K + x(t) C_D} \tag{1}$$

Here: K - is the area of the control electrode, C_D - is the capacitance of the dielectric layer, ε - is the dielectric constant of the semiconductor, ε_0 - is the electric constant, and $x(t)$ - is the time dependence of the width of the space charge region (SCR) of the semiconductor. The value of C_D - is determined by the high-frequency current-voltage characteristic. The quantity $C(t)$ can be found, for each instant t, from the experimental relaxation characteristic of the MIS structure, using the expression (1) and (2):

$$x = \left(x_0 + \frac{S}{A} \right) \exp\left(-\frac{A}{N} t \right) - \frac{S}{A} \tag{2}$$

Here: x - is the thickness of the space-charge layer of semiconductor of the MIS structure; x_0 - is the initial thickness of this layer; A - is the rate of generation of charge carriers in the bulk of semiconductors; S - is the rate of surface generation of charge 0063arriers; N - is the concentration of the dopant[13].

The resulting calculated time dependence of the width of the SCR can be used to determine the values of the velocity of surface and of charge carriers when compared with the experimental dependence[14].

To study the energy spectrum of bulk states localized in silicon[15], the identification technique described in was used, for which Schottky type Au-n-Si diodes were fabricated by chemical removal of the glass layer and vacuum deposition of Au.

4. THE RESULTS AND DISCUSSIONS

On drawing 1 is brought C-V feature (normalized to value of the capacities layer flow) of one of the under investigation structures, measured in the dark, on frequency 150 kHz before influence by ultrasound - a dependency 1 and after influence (the frequency 2,5 mHz power 0,5 Vt, in current 20 minutes) - a dependency 2. It is seen that after influence by ultrasound, C-V feature moves aside negative voltages and not vastly changes its form. The parallel shift C-V features of the structures MIS (made on base of the semiconductor n - a type to conductivities) aside negative voltages points to formation positive charge in structure glass.

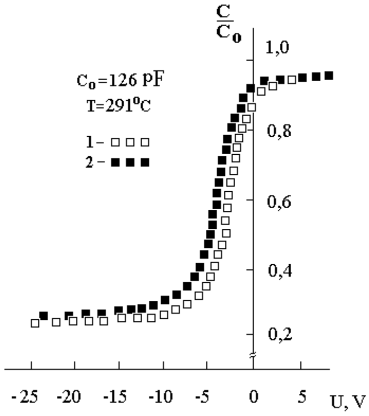

Figure 1. Experimental C-V charactericтisc of the one of investigated structures before action of ultrasonic irradiation 1, and aftear influence 2

But change the form C-V features of such structures, is indicative of increase the charge of the surface conditions, which are recharged when change the value of the put voltage. Presence of the rolling charge in structure leaden - a boron - silicate flow is conditioned localization, injection from semiconductor, electron in approach easy polarization ions lead and agglomeration them on potential barrier of the enabling the crystalline phase. In our opinion, the main reason, bring about increase the positive charge, can be a change the height potential barrier between enabling the crystalline phase. Really, reduction of the height potential barrier brings about that incorporated by attached voltage, from semiconductor electrons, not localizing in greater amount in potential pit, when change the polarities of the voltage, return back in volume of the semiconductor substrate[5].

For confirm this hypothesis the ultrasound effects were measured at different temperatures (-10^0C - $+ 50^0C$) and frequencies (100 kHz - 1MHz) in dielectrics. The comparison of the obtained thermal - frequency connections in all the measured constructions is allows to estabilish that the dielectric loss tangent have the characteristic maximum[16]. In ultrasound structures, the relaxation maximum of the dielectric losses decreases and becomes more pronounced. Such a change in the relaxation maximum also shows an increase in the magnitude of the moving charges in the glass structure [17].

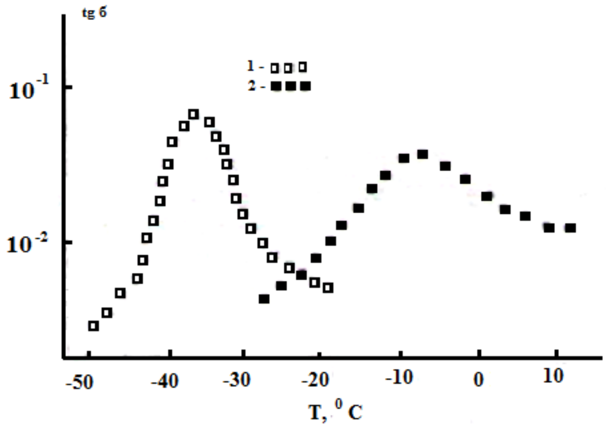

Figure 2. Dependence of the tangent of the dielectric loss angle on temperature. Structure without (1) and after (2) ultrasonic irradiation.

The values of the velocities of the volume (A) and surface (S) generation method of optimal choice using formulas (1) and (2) and the dependence of the width of the [18]. $A=9\bullet10^{13}s^{-1}sm^{-3}$, $S=4\bullet10^{9}s^{-1}sm^{-3}$. There is a correspondence with the experimental results with the calculations in the dependence (3-figure) of the relaxation of the vessel with the values of A and S.

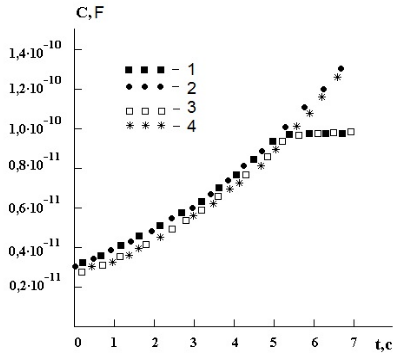

Figure 3. The experimental (1.3) and theoretical (2.4) dependences of the relaxation of the capacitance of the investigated strucutres: 3 and 4 are control, 1 and 2 are ultrasonically exposed.

The probability of calculating the calculated connection from the experimental to the end of the relaxation process is that the inversion increases with the charge level and increases the likelihood of retrieval of generated chargers[19]. For similar samples, however, under the influence of ultrasound, the capacitance relaxation is given in connection 3[20]. From these links, it is clear that the calculated (2.4) and experimental (1.3) connections are well-suited to the values $A = (8\text{-}9)\cdot10^{13}s^{-1}cm^{-3}$, $S=(1\text{-}2)\cdot10^{9}s^{1}sm^{-2}$. In our case, this situation indicates that energy intake of semiconductor concentration centers is practically unchanged as a result of processing at ultrasonic values and decreases the surface generation rate ($S=4\cdot10^{9}s^{-1}sm^{-2}$, $S=(1\text{-}2)\cdot10\ s^{-1}sm^{-\ 2}$ ultrasound samples)[21]. In order to confirm this assumption, the glass layers were removed from the ultrasound effectively by the chemical method (with formic acid vapor treatment) and the Au-n-Si type Shottky diode was prepared[22]. Then the method of isothermal relapse of the capacitance determined the concentration of localized centers of power distribution and diode base[23]. Analysis of the results shows the following. In all the Shotki diodes, under the control of both ultrasound effects[24], the energy state of the centers (*E_V-0,27эВ and E_C-0,54эВ*, as well as their concentration n = $(3\text{-}5)\cdot10^{12}sm^{-3}$) is practically the same (for different diodes the value of the value is 5-7%) and is lies in the error of the experiment. In our opinion, this given ultrasound does not affect to parameters of centers of volumetric generation, in results as chargers do not affect the speed of the volume generation[25]. Immediate measurements of the density of the surface state by the high-frequency volt-farad method have shown (at a frequency of 150 kHz, from -50^{0}S to -180^{0}S) (Fig.4) that in structures subjected to ultrasound, the distribution of intrinsic density over the width of the semiconductor zone width decreases in comparison with the control samples[16]. Especially this decline is very noticeable at energy values greater than E = E_c-0.4 eV

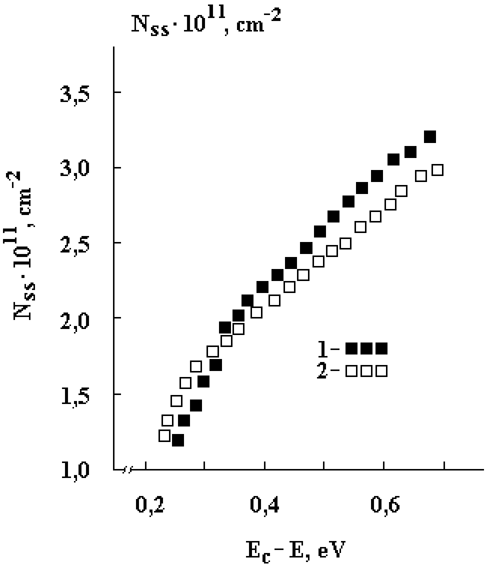

Figure 4. Distributions are the integral density of surface states for the investigated structures (1 - control structure, 2 - structure subjected to ultrasound).

It should be noted that similar reduction of localized density in the semiconductor - dielectric boundary phase section was observed in all aspects of the MIS structures, which was observed to decrease the rate of surface generation[26]. In order to clarify this state, was determined change of the rate of surface generation using the formula (1) and (2) is shown in Fig. 5, whereas in the MIS structures the surface generated speeds in ultrasonic waves are relatively small compared to the test sample, and the transition time to the surface generator is significantly flattened[27].

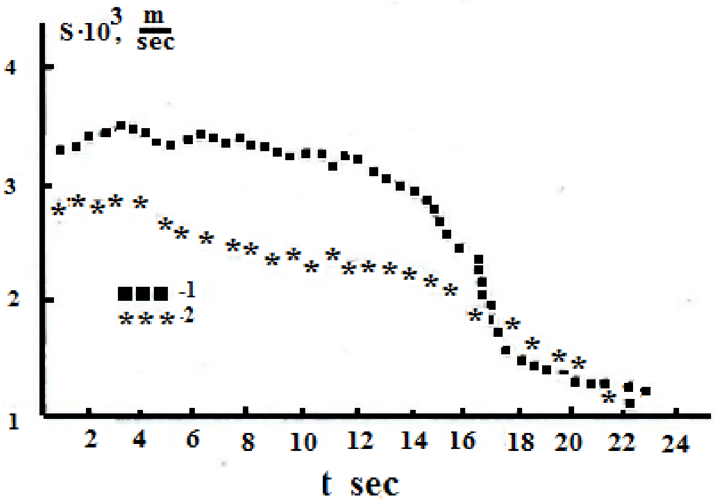

Figure 5. Dependence of surface generation rate on time s(t). (For a sample with a MIS structure 1-dependence and for MIS structures with ultrasonic action 2-dependence are corresponds)

The spectral distribution of the density of surfaces along the silicon zone is almost unchanged after the ultrasound effect, so that ultrasound in metal-glass-semi-conductive structures leads to the change in the structure of glass layers at the boundary layer of the semiconductor glass separation[28]. Separation of crystals in the glass content may lead to the decrease in the width and number of boundary phases[29], while the decrease in the rate of the external genera- tion and its time-varying variation. To investigate this hypothesis, the Al layer, which performs the chemo-electrode service from the MIS, has been removed and the surface layers of the anticholic vapors are removed. Then the microflora of the glass surface was obtained.

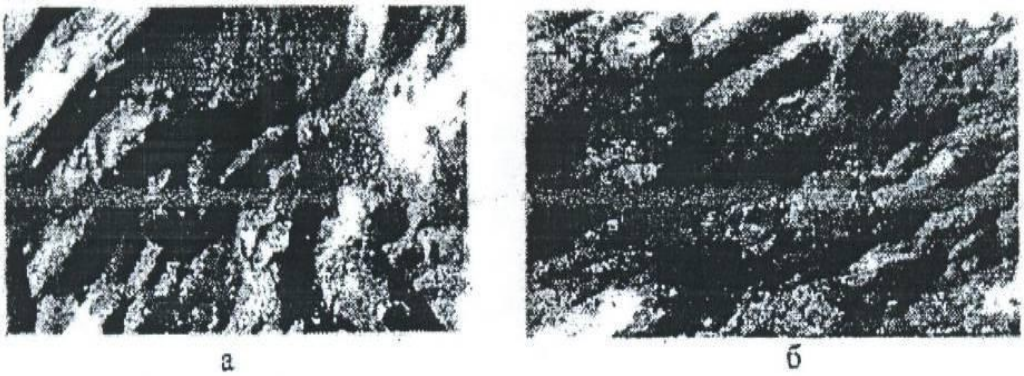

Figure 6. Microphotography of the surface of the investigated structures
a) before ultrasonic exposure
b) after ultrasonic with a power P = 0.5 W/cm^2 for t=90 minutes

In Figure 6 shows the magnification of the glass surface of the two enlarged (2800 times) structures. Comparison of images suggests that, in ultrasound structures, the glass surface is less sensitive to a variety of additives and non-strangers[23].

5. CONCLUSION

Based on these results, when influenced at a frequency of 2.5 MHz, with a power of 0.5 W for 40 minutes, on the structures of Al-n-Si-glass-Al leads to a decrease in the integrated density of localized electronic states on the boundary of interphase of semiconductor - glass, and the surface electronic state of the semiconductor do not affect the energy spectrum, and the rate of surface generation decreases. Ultrasonic processing can lead to the improvement of the recombinative properties of the genera of the silicate glass and silicon boundary phase phase in the order shown.

6. REFERENCES

[1] J. Goraus, J. Kubacki, J. Czerniewski, and M. Fijałkowski, "Cisplatin - A new wide bandgap semiconductor," *J. Alloys Compd.*, vol. 817, Mar. 2020, doi: 10.1016/j.jallcom.2019.153270.

[2] L. Ma, P. Bocchini, and V. Christou, "Fragility models of electrical conductors in power transmission networks subjected to hurricanes," *Struct. Saf.*, vol. 82, Jan. 2020, doi: 10.1016/j.strusafe.2019.101890.

[3] L. A. Galindo, G. Gozzi, L. Fugikawa-Santos, R. M. Faria, F. C. Lavarda, and A. Batagin-Neto, "Investigation of the polymer-salt interactions in polymeric light emitting electrochemical cells: Electronic structure calculations and experimental studies," *Org. Electron.*, vol. 79, Apr. 2020, doi: 10.1016/j.orgel.2020.105629.

[4] D. A. Smolyakov *et al.*, "Influence of metal magnetic state and metal-insulator-semiconductor structure composition on magnetoimpedance effect caused by interface states," *Thin Solid Films*, vol. 671, pp. 18–21, Feb. 2019, doi: 10.1016/j.tsf.2018.12.026.

[5] S. K. Srivastava, P. Magudapathy, P. Gangopadhyay, S. Amirthapandian, S. Bera, and A. Das, "Ag nanoparticles in compound metal oxide semiconductors: Syntheses and characterizations," *Thin Solid Films*, vol. 681, pp. 86–92, Jul. 2019, doi: 10.1016/j.tsf.2019.04.039.

[6] Y. B. Saddeek, K. A. Aly, and S. A. Bashier, "Optical study of lead borosilicate glasses," *Phys. B Condens. Matter*, vol. 405, no. 10, pp. 2407–2412, May 2010, doi: 10.1016/j.physb.2010.02.055.

[7] D. O. Kim *et al.*, "Novel high-k gate dielectric properties of ultrathin hydrocarbon films for next-generation metal-insulator-semiconductor devices," *Carbon N. Y.*, vol. 158, pp. 513–518, Mar. 2020, doi: 10.1016/j.carbon.2019.11.019.

[8] M. Dou, J. Wang, B. Gao, C. Xu, and F. Yang, "Photocatalytic difference of amoxicillin and cefotaxime under visible light by mesoporous g-C3N4: Mechanism, degradation pathway and DFT calculation," *Chem. Eng. J.*, vol. 383, Mar. 2020, doi: 10.1016/j.cej.2019.123134.

[9] A. Madheshiya, K. K. Dey, M. Ghosh, J. Singh, and C. Gautam, "Synthesis, structural, optical and solid state NMR study of lead bismuth titanate borosilicate glasses," *J. Non. Cryst. Solids*, vol. 503–504, pp. 288–296, Jan. 2019, doi: 10.1016/j.jnoncrysol.2018.10.009.

[10] K. Vijaya Babu and S. Cole, “Spectral and luminescence properties of Sm3+ doped sodium lead alumino borosilicate glasses,” in *Materials Today: Proceedings*, 2018, vol. 5, no. 13, pp. 26440–26449, doi: 10.1016/j.matpr.2018.08.098.

[11] M. E. Sánchez Vergara, V. Medel, C. Rios, and R. Salcedo, “Doping of molecular materials based on ferrocene and the study of their properties as organic semiconductors for their application in optoelectronic devices,” *J. Mol. Struct.*, vol. 1193, pp. 365–372, Oct. 2019, doi: 10.1016/j.molstruc.2019.05.053.

[12] C. Zhao, K. E. Knisely, and K. Grosh, “Design and fabrication of a piezoelectric MEMS xylophone transducer with a flexible electrical connection,” *Sensors Actuators, A Phys.*, vol. 275, pp. 29–36, Jun. 2018, doi: 10.1016/j.sna.2018.03.038.

[13] S. A. Khan *et al.*, “New physical insight into crystal structure, luminescence and optical properties of YPO4:Dy3+\Eu3+\Tb3+ single-phase white-light-emitting phosphors,” *J. Alloys Compd.*, vol. 817, Mar. 2020, doi: 10.1016/j.jallcom.2019.152687.

[14] M. Kantner, “Generalized Scharfetter–Gummel schemes for electro-thermal transport in degenerate semiconductors using the Kelvin formula for the Seebeck coefficient,” *J. Comput. Phys.*, vol. 402, Feb. 2020, doi: 10.1016/j.jcp.2019.109091.

[15] I. Elahi, S. M. Alay-e-Abbas, S. Nazir, A. Shaukat, and M. N. Tahir, “Evaluation of thermodynamics and p-type ferromagnetism of C, Si and Ge doped ZnX (X = S, Se and Te) semiconductors,” *J. Magn. Magn. Mater.*, vol. 477, pp. 249–257, May 2019, doi: 10.1016/j.jmmm.2019.01.072.

[16] Y. Meng *et al.*, “Novel high ionic conductivity electrolyte membrane based on semiconductor La0.65Sr0.3Ce0.05Cr0.5Fe0.5O3-Δ for low-temperature solid oxide fuel cells,” *J. Power Sources*, vol. 421, pp. 33–40, May 2019, doi: 10.1016/j.jpowsour.2019.02.100.

[17] E. A. Franceschini, A. Hainer, and A. E. Lanterna, “Niobium-based semiconductor electrodes for hydrogen evolution reaction,” *Int. J. Hydrogen Energy*, vol. 44, no. 60, pp. 31940–31948, Dec. 2019, doi: 10.1016/j.ijhydene.2019.10.101.

[18] V. B. Bogevolnov, A. M. Yafyasov, and I. Y. Pavlovskaya, “Proton transfer as a feedback in the semiconductor-electrolyte interface,” *Surf. Sci.*, vol. 691, Jan. 2020, doi: 10.1016/j.susc.2019.121508.

[19] A. G. Xie, Y. Yu, C. N. Song, and Y. Y. Chen, “Study of secondary electron emission from semiconductors induced by electrons from 20 eV to 800 eV and surface state of semiconductors,” *Results Phys.*, vol. 15, Dec. 2019, doi: 10.1016/j.rinp.2019.102724.

[20] T. A. Krouskop, T. M. Wheeler, F. Kallel, B. S. Garra, and T. Hall, “Elastic moduli of breast and prostate tissues under compression,” *Ultrason. Imaging*, 1998, doi: 10.1177/016173469802000403.

[21] M. O. Erdal, A. Kocyigit, and M. Yıldırım, “The rate of Cu doped TiO2 interlayer effects on the electrical characteristics of Al/Cu:TiO2/n-Si (MOS) capacitors depend on frequency and voltage,” *Microelectron. Reliab.*, vol. 106, Mar. 2020, doi: 10.1016/j.microrel.2020.113591.

[22] Z. El-Moussawi, A. Nourdine, H. Medlej, T. Hamieh, P. Chenevier, and L. Flandin, “Fine tuning of optoelectronic properties of single-walled carbon nanotubes from conductors to semiconductors,” *Carbon N. Y.*, vol. 153, pp. 337–346, Nov. 2019, doi: 10.1016/j.carbon.2019.07.023.

[23] J. Zhou, X. M. Long, and H. J. Luo, "Spectrum optimization of light-emitting diode insecticide lamp based on partial discharge evaluation," *Meas. J. Int. Meas. Confed.*, vol. 124, pp. 72–80, Aug. 2018, doi: 10.1016/j.measurement.2018.03.073.

[24] W. D. O'Brien, "Ultrasound-biophysics mechanisms," *Progress in Biophysics and Molecular Biology*. 2007, doi: 10.1016/j.pbiomolbio.2006.07.010.

[25] S. Sun, Q. Yang, J. Ma, A. J. Ferré, and W. Yan, "Hierarchical planning of PEV charging facilities and DGs under transportation-power network couplings," *Renew. Energy*, vol. 150, pp. 356–369, May 2020, doi: 10.1016/j.renene.2019.12.097.

[26] R. Xu *et al.*, "Scalable fabrication of geometry-tunable self-aligned superlattice photonic crystals for spectrum-programmable light trapping," *Nano Energy*, vol. 58, pp. 543–551, Apr. 2019, doi: 10.1016/j.nanoen.2019.01.074.

[27] A. Vallet, L. Chusseau, F. Philippe, and A. Jean-Marie, "Markov model of quantum fluctuations at the transition to lasing of semiconductor nanolasers," *Phys. E Low-Dimensional Syst. Nanostructures*, vol. 105, pp. 97–104, Jan. 2019, doi: 10.1016/j.physe.2018.08.028.

[28] J. Feng *et al.*, "Non-oxide semiconductors for artificial photosynthesis: Progress on photoelectrochemical water splitting and carbon dioxide reduction," *Nano Today*, vol. 30. Elsevier B.V., 01-Feb-2020, doi: 10.1016/j.nantod.2019.100830.

[29] Y. Wan *et al.*, "Preparation of inverse opal titanium dioxide for photocatalytic performance research," *Opt. Mater. (Amst).*, vol. 96, Oct. 2019, doi: 10.1016/j.optmat.2019.109287.